Defining the Physical Gate of a Mechanosensitive Channel, MscL, by Engineering Metal-Binding Sites

Irene Iscla, Gal Levin, Robin Wray, Robert Reynolds, and Paul Blount
Department of Physiology, University of Texas-Southwestern Medical Center, Dallas, Texas

ABSTRACT The mechanosensitive channel of large conductance, MscL, of *Escherichia coli* is one of the best-studied mechanosensitive proteins. Although the structure of the closed or "nearly-closed" state of the *Mycobacterium tuberculosis* ortholog has been solved and mechanisms of gating have been proposed, the transition from the closed to the open states remains controversial. Here, we probe the relative position of specific residues predicted to line the pore of MscL in either the closed state or during the closed-to-open transition by engineering single-site histidine substitutions and assessing the ability of Ni^{2+}, Cd^{2+} or Zn^{2+} ions to affect channel activity. All residues predicted to be within the pore led to a change in channel threshold pressure, although the direction and extent of this change were dependent upon the mutation and metal used. One of the MscL mutants, L19H, exhibited gating that was inhibited by Cd^{2+} but stimulated by Ni^{2+}, suggesting that these metals bind to and influence different states of the channel. Together, the results derived from this study support the hypotheses that the crystal structure depicts a "nearly closed" rather than a "fully closed" state of MscL, and that a clockwise rotation of transmembrane domain 1 occurs early in the gating process.

INTRODUCTION

Mechanosensitive (MS) channels that gate in response to mechanical stress applied to the cell membrane or to cytoskeletal elements are proposed to play a central role in a variety of physiological processes including touch, hearing, balance, circulation, and osmoregulation (Hamill and Martinac, 2001). Four MS channel activities have been characterized in *Escherichia coli*: the mechanosensitive channel of large conductance, MscL; the mechanosensitive channel of smaller conductance, MscS; the mechanosensitive channel of mini-conductance, MscM; and the K^+-regulated mechanosensitive channel, MscK (Berrier et al., 1996; Li et al., 2002; McLaggan et al., 2002). The MscL and MscS channels appear to play a fundamental role in protecting the cell from an acute decrease in osmolarity of the environment since the double null shows a dramatic decrease in viability upon such an osmotic downshock (Levina et al., 1999). Because they can be purified, reconstituted into synthetic lipid membranes, and remain functional (Häse et al., 1995; Blount et al., 1996a), it appears that both MscL and MscS directly sense and respond to bilayer tension.

Thus far, the best-studied MS protein is MscL. A pivotal point in the study of this channel occurred when the crystal structure of the MscL homolog from *Mycobacterium tuberculosis* (Tb MscL) was resolved to 3.5 Å by x-ray crystallography (Chang et al., 1998). This structure revealed a homopentameric channel. Each subunit consists of two transmembrane (TM) α-helices that are tilted by $\sim$35° with respect to the membrane normal; both the N- and C-termini are cytoplasmic. The five TM1s appear packed together in a right-handed bundle forming the permeation pathway, whereas the TM2 helices are on the periphery, presumably interacting with membrane lipids. The narrowest region of the pore lies in the cytoplasmic half of TM1 with a constriction point of $\sim$4 Å. Given that the size of the open pore, estimated by conductance and molecular sieving experiments, is thought to be $>$30 Å (Cruickshank et al., 1997), the crystal structure would depict a closed or nearly-closed state of the channel (Chang et al., 1998).

The importance of the first half of TM1 for MscL gating was suggested by random and site-directed mutageneses, combined with whole-cell physiology and electrophysiological studies. Substitution of hydrophobic residues in this region with polar or charged amino acids typically leads to channel activities with a decreased threshold to membrane tension when assayed by patch clamp, and a gain-of-function (GOF) in vivo phenotype in which cell growth is impaired and/or viability reduced (Blount et al., 1996b; Ou et al., 1998; Yoshimura et al., 1999; Maurer and Dougherty, 2003). These data suggested that several of these residues, which in the crystal structure appear buried, are exposed to an aqueous environment, presumably the opening lumen of the channel, upon gating.

Although determination of a crystal structure advanced the field tremendously, several questions remain. One is whether the resolved structure corresponds to the fully closed state of the channel. The crystal structure implies that the analog of *E. coli* V23 is the constriction point of the pore, but a more recent study suggests it may be G26 (Levin and Blount, 2004). Other questions concern the structural changes that occur during the transition from the closed to the open state; two

Submitted July 15, 2004, and accepted for publication August 23, 2004.

Address reprint requests to Paul Blount, Dept. of Physiology, University of Texas-Southwestern Medical Center, 5323 Harry Hines Blvd., Dallas, TX 75390-9040. Tel.: 214-648-8445; Fax: 214-648-4771; E-mail: Paul.Blount@UTSouthwestern.edu.

0006-3495/04/11/3172/09 $2.00

doi: 10.1529/biophysj.104.049833

models have been proposed. Both agree that the transmembrane domains tilt relative to the membrane plane upon channel opening. However, the first model, proposed from structural modeling and supported by disulfide trapping experiments (Sukharev et al., 2001a,b; Betanzos et al., 2002), suggests that TM1 undergoes a slight counterclockwise rotation during gating. In the second model, supported by electron paramagnetic resonance (EPR) spectroscopy (Perozo et al., 2002), TM1 undergoes a full 110° rotation in the opposite, clockwise direction during this transition. The two models predict an entirely different set of residues to line the open pore.

To determine the exposure of a single residue to the open pore upon gating, Batiza et al. (2002) developed an in vivo assay relying on the ability of a charge introduced into the pore lumen to effect a GOF phenotype. Using an L19C-mutated channel, the accessibility of the substituted residue to the aqueous environment was assayed by determining the viability of cells subsequent to exposure to a large charged sulfhydryl reagent, [2(triethylammonium)ethyl] methanethiosulfonate (MTSET). When the reagent was added simultaneously with an osmotic downshock, which gated the channel, the binding of the charged sulfhydryl led to channel misgating, thus causing cell death (Batiza et al., 2002). Utilizing a cysteine-scanning library, the aqueous accessibility of every residue in both transmembrane domains was tested in a similar assay (Bartlett et al., 2004). An additional set of residues that were predicted to be exposed upon osmotic treatment, provided support for the model based upon the EPR studies.

Here, we utilize an independent approach to test for the availability and proximity of residues predicted by current models to line the opening pore. We have substituted candidate residues with histidine and tested for the ability of these residues to form metal-binding sites within the homopentameric complex. Previous studies have shown that metals can bind to histidine- or cysteine-containing channels and influence their function. In several reported cases the coordination of the metal by multiple residues has led to high-affinity binding sites that stabilize the channel in specific conformations (Liu et al., 1997; Holmgren et al., 1998; Rothberg et al., 2002, 2003; Webster et al., 2004). We use this approach to test the accessibility and relative position of specific residues in the closed and opening *E. coli* MscL channel. We have substituted single residues at R13, L19, G22, V23, I24, G26, and F29 with histidine and tested the ability of Ni^{2+}, Cd^{2+}, or Zn^{2+} to alter the gating properties of the mutated channels by patch clamp. A change in pressure threshold was observed in many of these mutated channels. The changes were histidine-mutant specific, varied at different residue locations, and showed the pH-dependence predicted for metal binding to histidines residing within a protein, strongly suggesting that this influence of metals on channel activity is a direct effect of metal ion binding by the substituted histidines. The data support G26 as the constriction point in the closed channel and the clockwise rotation of TM1 upon gating predicted from EPR studies (Perozo et al., 2002).

MATERIALS AND METHODS

Strains and cell growth

E. coli FRAG-1 (Epstein and Davies, 1970) derivative strain, MJF465 Δ*mscL::Cam*, Δ*yggB*, Δ*kefA::Kan* (Levina et al., 1999), and *E. coli* strain PB104 (Δ*mscL::Cm*) (Blount et al., 1996a,b), were used as hosts for the pB10 expression constructs (Blount et al., 1996a,b; Ou et al., 1998; Moe et al., 2000). PB104 was used for assessing in vivo GOF phenotypes and for electrophysiological analysis in which MscS was used as an internal control, whereas in experiments in which absolute pressure values (pre- and posttreatment) were compared, MJF465 was used as the host. Cultures were routinely grown in Lennox Broth (LB) plus ampicillin (100 μg/ml) in a shaker-incubator at 37°C, rotated 250 cycles per minute. Expression was induced by addition of 1 mM isopropyl-β-D-thiogalactopyranoside (IPTG). Growth curves at different pH values were performed in citrate-phosphate medium containing (per liter) 8.58 g Na_2HPO_4, 0.87 g K_2HPO_4, 1.34 g citric acid, 1 g $(NH_4)_2SO_4$, 0.001 g thiamine, 0.1 g $MgSO_4{\cdot}7H_2O$, 0.002 g $(NH_4)_2SO_4{\cdot}FeSO_4{\cdot}6H_2O$, and 0.2% glucose plus ampicillin (100 μg/ml). Cultures inoculated from a single colony were grown overnight in citrate-phosphate medium (pH 7.0), diluted 1:100 to 30 ml citrate-phosphate medium of indicated pH and, when the optical density of the culture at 600 nm (OD_{600}) was ~0.2, 1 mM IPTG was added. Culture growth (OD_{600}) was recorded at 30-min intervals.

Mutagenesis

Site-directed mutagenesis of *mscL* was accomplished by PCR, using QuikChange site-directed mutagenesis kit (Stratagene, La Jolla, CA). Briefly, oligonucleotide primers were designed that incorporated the desired codon change accompanied by 12–18 base-pair flanking sequences on each side. The wild-type (WT) *E. coli* MscL in the expression vector pB10b was used as a template. The final verification of the mutation was ascertained by sequencing in both directions.

Electrophysiology

E. coli giant spheroplasts were generated and used in patch-clamp experiments as described previously (Blount and Moe, 1999). Excised, inside-out patches were examined at room temperature under symmetrical conditions using a buffer comprised of 200 mM KCl, 90 mM $MgCl_2$, 10 mM $CaCl_2$, and 5 mM HEPES with different pH values achieved by addition of KOH or HCl. When a single concentration was used, $NiCl_2$, $CdCl_2$, or $ZnCl_2$ (Sigma, St. Louis, MO) was dissolved in patch buffer to their final concentration and perfused into the bath solution. For concentration curves, a solution at the highest concentration tested was made and aliquots of this stock were added to the recording chamber solution and mixed to achieve the desired final concentration. Measurements were made 2 min subsequent to treatment (or wash). Note that we have reported the total concentration of metal ion; free-ion concentrations are several-fold lower due to the binding to Cl^- (Rothberg et al., 2003).

Recordings were performed at −20 mV (positive pipette). Data were acquired at a sampling rate of 20 kHz with a 5-kHz filter using an AxoPatch 200B amplifier in conjunction with Axoscope software (Axon Instruments, Union City, CA). A piezoelectric pressure transducer (World Precision Instruments, Sarasota, FL) was used to measure the pressure throughout the experiments. The MscL threshold was defined as the pressure at which openings were observed at least every 0.5–2 s. Measurements before and after treatment were compared. To compare channel tension thresholds

between mutated and wild-type channels in the absence of metals, the tension threshold was expressed as a fraction of the threshold for MscS, which was used as an internal control as previously described (Blount et al., 1996b, 1999; Ou et al., 1998).

RESULTS

Metals bind specifically to clustered histidines of the MscL R13H mutant

The R13 residue within the *E. coli* MscL channel has been found to have several interesting properties. R13C confers a GOF phenotype, spontaneously forms disulfide bridges in excised patches, and, when exposed to the sulfhydryl reagent MTSET, its GOF phenotype is partially remediated (Bartlett et al., 2004; Levin and Blount, 2004). These data imply an interesting correlation between the charged state of this residue and the dynamics of this region during gating, suggesting it as a prime candidate for testing the mutated MscL channel for metal-induced functional changes. Preliminary experiments with R13C demonstrated that an 80% increase in stimulus was necessary to gate the channel when 500 μM Cd^{2+} was added to the bath of an excised patch (not shown). However, because R13C spontaneously forms disulfide bridges, channel activity could only be observed routinely in the presence of dithiothreitol, thus complicating the interpretation. We therefore generated the R13H mutant, which retains the ability to bind metals but will not form intersubunit disulfide bridges.

The function of R13H was found to be pH-dependent in vivo. As seen in Fig. 1, *E. coli* cells expressing this mutant grew similar to those expressing wild-type MscL at lower pH; however, attenuated growth was observed at higher pH. The channel activity was characterized in giant spheroplasts by patch clamp. The channels had ''flickery'' kinetics (shorter open dwell time) at all pHs assayed (not shown). As discussed below, shorter dwell time is one of the properties previously reported for MscL channels with mutations near the pore (Ou et al., 1998; Yoshimura et al., 1999; Maurer and Dougherty, 2003; Levin and Blount, 2004). Consistent with the in vivo observations, patch-clamp results confirmed that the channel was more sensitive to mechanical stimuli at higher pH, whereas no difference was noted in the pressure required to open the wild-type versus the R13H mutant at pH 6.0 (220 $\pm$ 30 vs. 230 $\pm$ 30 mm Hg; $p = 0.7$; $n \geq 6$). Shifting the bath to pH 9.0 led to a decrease in the threshold pressure for both the wild-type and the R13H mutant MscL. However, this decrease in threshold was more profound for R13H than for wild-type MscL (28 $\pm$ 3% vs. 15 $\pm$ 3%, $p < 0.02$). These pH effects were reversible (not shown). These data suggest that removing the charge at the R13 position leads to a channel that misgates in vivo, thus conferring a GOF phenotype; reconstitution of this charge increases the threshold for the channel, and suppresses the phenotype.

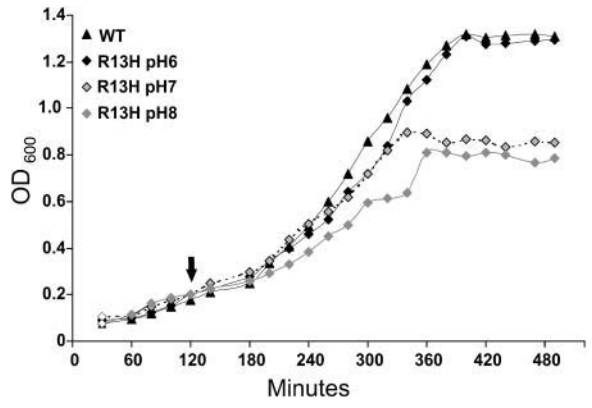

FIGURE 1 R13H MscL confers a GOF growth phenotype in a pH-dependent manner. The *E. coli* pB104 *mscL*-null strain transformed with the expression vector pB10b containing either WT or R13H-mutated MscL were grown in citrate-phosphate media at pH 6, pH 7, or pH 8. The growth of bacterial cultures was monitored every 30 min by measuring their optical density (OD_{600}). Expression of the channel was induced at minute 120, as indicated by the arrow, by addition of 1 mM IPTG. Bacteria expressing WT MscL showed similar growth rates at all the pHs tested; an average trace is shown.

Consistent with the preliminary results with R13C (above), R13H gating was affected by the presence of Ni^{2+} or Cd^{2+} ions (Fig. 2). An increase in pressure threshold was observed. This influence on channel activity was observed at concentrations in the tens to hundreds of micromoles and achieved saturation at ~2 mM (Fig. 3 *A*). This effect was reversible upon perfusion with a solution free of the metal ions (Fig. 3 *B*). Neither metal affected the pressure threshold of the wild-type channel. These data suggest a direct interaction of the metals with the substituted histidines exposed to the channel lumen, as opposed to an influence of these divalent cations on lipid fluidity or other indirect effects.

The metal-dependent increase in channel threshold was also found to be strongly influenced by pH. Metals bind histidine-containing proteins preferentially at higher pH where these residues are electrically neutral (Cherny and DeCoursey, 1999; Paddock et al., 2003). For R13H, the increase in pressure threshold observed in the presence of Cd^{2+} was six times greater at pH 8.0 than at pH 6.0. Similarly, a threefold increase was observed for Ni^{2+} (Fig. 3 *C*) ($p < 0.001$ by unpaired Student's *t*-test for both Ni^{2+} and Cd^{2+}). That this change occurs near the expected pKa value for a histidine residue within a protein further supports the hypothesis that the metal ions are directly interacting with the histidine residues.

Defining residues that line the pore by utilizing a metal-binding assay

A recent study has predicted several specific residues, L19, G22, V23, I24, and G26, to face the channel lumen (Bartlett et al., 2004). To determine their exposure upon gating, we

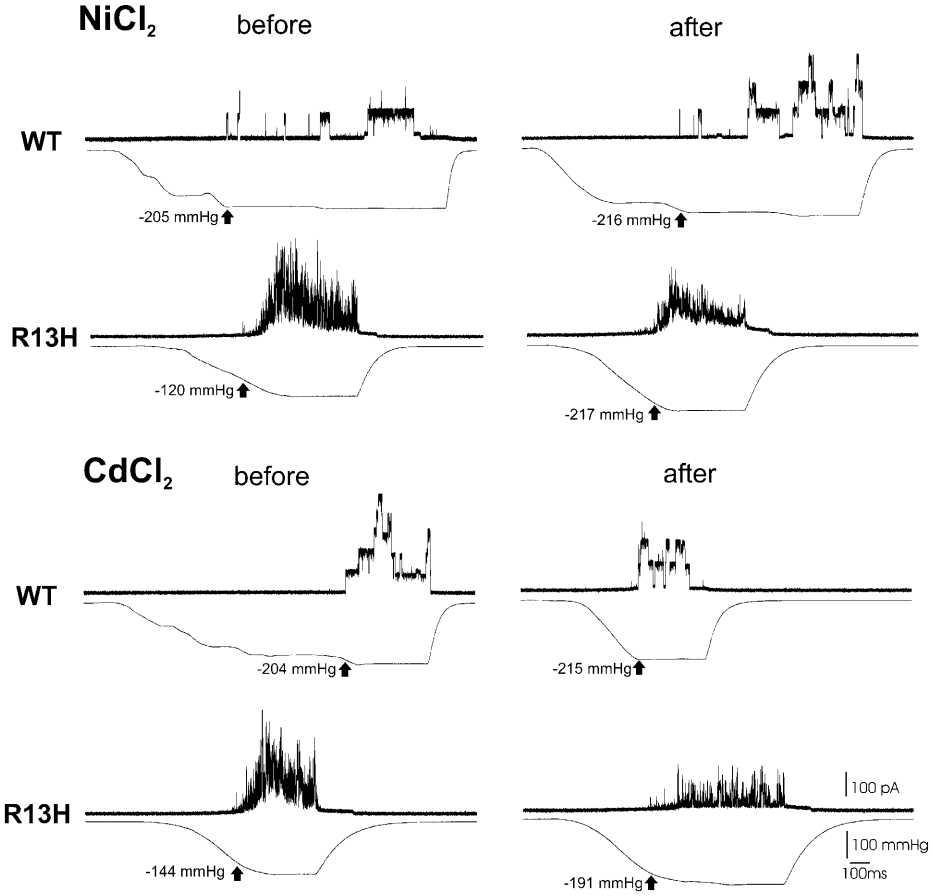

FIGURE 2 Metal ions increase the pressure threshold of the R13H MscL mutant. WT and R13H-mutated MscL were expressed in the *E. coli* MJF465 *mscS*, *mscK*, and *mscL* triple-null strain, and the resulting MS channel activities were measured by patch clamp at pH 8.0. Representative traces before (*left*) and after (*right*) addition of 5 mM $NiCl_2$ (*top*) or $CdCl_2$ (*bottom*) solutions to the bath are shown; the upper trace shows channel activity while the lower trace depicts the pressure applied to the patch. Arrows indicate the threshold pressure.

sequentially substituted each residue with histidine and assayed for metal-induced changes in activity by patch clamp. In in vivo experiments, each of these histidine mutants was found to confer a slowed-growth GOF phenotype. Further, patch-clamp analysis demonstrated that these channels indeed have a lower gating threshold than wild-type MscL. When expressed in PB104, a strain that expresses MscS, the ratio of the pressure threshold of MscL to that of MscS ranged from 0.72 to 1.22 for all of the above mutated channels, significantly lower than the wild-type value of 1.48 ($p \leq 0.01$ for all mutants when compared to wild-type using Student's *t*-test). These wild-type ratios are consistent with values published previously (Blount et al., 1996b, 1999; Ou et al., 1998). In contrast to R13H, none of these histidine mutants showed any measurable pH modulation in vivo or in vitro (data not shown). Previous studies have demonstrated that the kinetics of wild-type MscL can be well fit to three open dwell times, of which two are >1 ms (Ou et al., 1998; Yoshimura et al., 1999; Levin and Blount, 2004). In contrast, all of the calculated open dwell times for the above mutants were consistently <1 ms. The GOF phenotypes, decreased membrane tension thresholds, and shorter dwell times are channel properties previously reported for MscL channels with mutations within the pore (Ou et al., 1998; Yoshimura et al., 1999; Maurer and Dougherty, 2003; Levin and Blount, 2004).

The G22H, V23H, I24H, and G26H mutants showed an increase in pressure threshold upon addition of Cd^{2+} or Ni^{2+} in the bath (Fig. 4, *top* and *middle*). Similar to R13H, this effect was reversible and was observed at pH 8.0, but not at pH 6.0 (not shown). Together, these data strongly suggest that the metals bind to electrically neutral histidines within the lumen of the channel and increase the energy required for gating. Because zinc is well characterized and binds to histidine with a higher affinity than Ni^{2+} or Cd^{2+} (Krizek et al., 1993), we also tested all mutants with this metal. As seen in Fig. 4 (*bottom*), Zn^{2+} not only gave results consistent with Cd^{2+} and Ni^{2+}, but yielded a larger effect (note the difference in scale of the *y* axis).

We also generated a histidine substitution at F29, a residue not predicted to be in the pore by Bartlett et al. (2004). Although this mutant did confer a slowed-growth GOF phenotype in vivo, it did not show a statistically significant decrease in membrane tension threshold (MscL/MscS pressure ratio of 1.30 ± 0.01 for F29, $n = 19$; for wild-type 1.48 ± 0.04, $n = 11$; $p = 0.056$); furthermore, in contrast to the histidine substitutions of residues predicted to line the pore an increase, rather than a decrease, in the open dwell time was

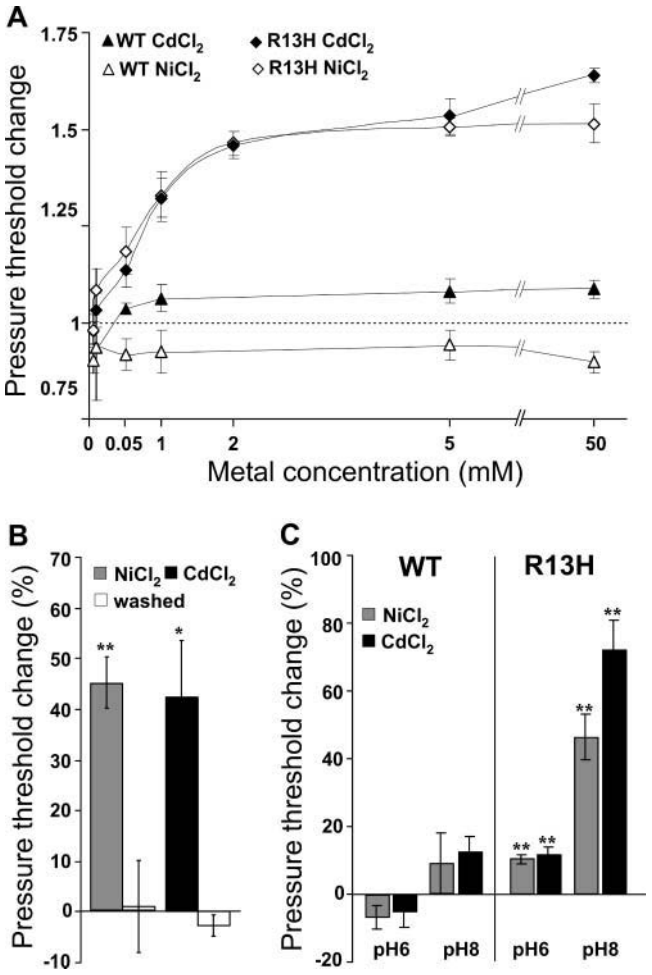

FIGURE 3 Metal binding to the R13H MscL mutant is saturable, reversible, and pH-dependent. (*A*) The change in the pressure needed to gate WT (*triangles*) and R13H (*diamonds*) MscL, as a function of metal ion concentration, is shown. Pressure thresholds for WT and R13H MscL were measured in patch-clamp experiments at increasing concentrations of Ni^{2+} or Cd^{2+} ions applied to the bath at pH 8.0. Error bars are the SEM of three or more independent experiments. (*B*) The changes in the pressure threshold of R13H MscL in the presence of 5 mM metal ions in the bath, and after wash, are shown (pH 8.0). Values are the ratio between the pressure thresholds ((after/before treatment) − 1), and are expressed as percentages. Error bars are the SEM of four or more independent experiments. (*C*) The changes in pressure threshold of WT and R13H MscL in the presence of 5 mM metal ions at pH 6.0 ($n = 12$) and pH 8.0 ($n = 7$) are shown. Error bars are SEM. $*p < 0.05$, $**p < 0.005$ from a paired Student's *t*-test, control versus treated.

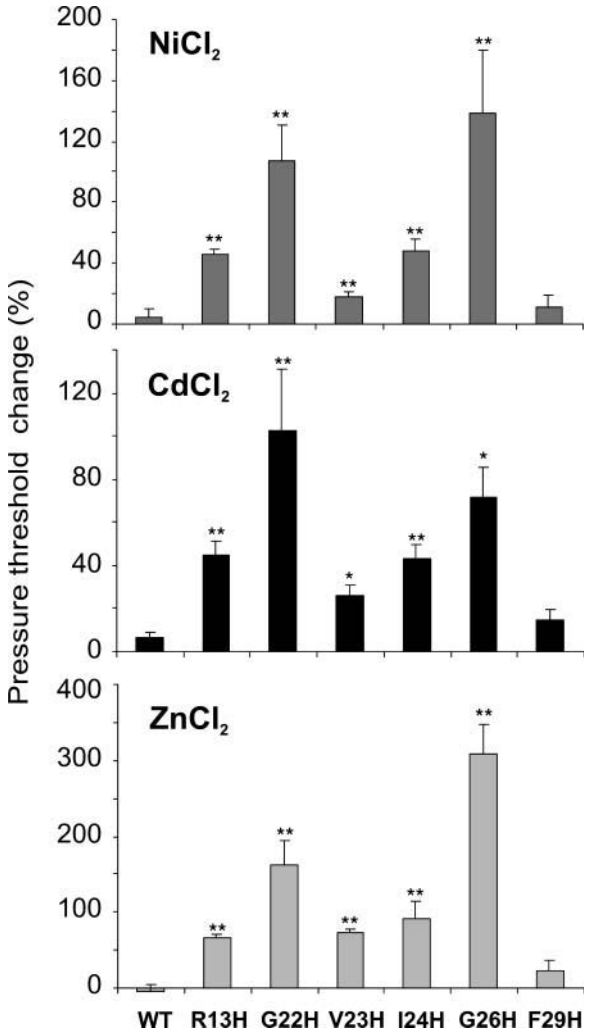

FIGURE 4 Histidine substitutions of residues predicted to be exposed to the lumen lead to channels that show increased threshold in the presence of metal ions; F29H, not predicted to be in the pore, does not. Percent increases in the pressure threshold of WT MscL and TM1 histidine mutants after perfusion of 5 mM Ni^{2+} (*top*), Cd^{2+} (*middle*), or Zn^{2+} (*bottom*) to the bath (pH 8.0) are shown. Error bars are the SEM of five or more independent experiments. $*p < 0.01$, $**p < 0.002$ from an unpaired Student's *t*-test, ratio of mutant (treated/control) versus ratio of wild-type MscL.

observed (τ_2 and τ_3 of 25 and 386 ms vs. 6 and 33 ms for wild-type; τ_1 is consistently <1.0 ms (Li et al., 2004)). Also in contrast to mutations at positions predicted to project into the pore, no significant changes in F29H channel properties in the presence of metals were observed (Fig. 4).

Defining the periplasmic pore constriction point

From previous studies, evidence exists that either V23 or G26 define the periplasmic constriction point of the closed homomultimeric MscL channel (Chang et al., 1998; Sukharev et al., 2001b; Levin and Blount, 2004). A residue forming the pore in this respect should better coordinate the metal, thus leading to a higher binding affinity. Because Zn^{2+} yielded the largest effects (see Fig. 4), we characterized the pressure-threshold changes of the V23H and G26H mutants at varying concentrations of this ion. As seen in Fig. 5 *A*, Zn^{2+} increased the pressure threshold of both histidine-mutated channels in a concentration-dependent manner; no significant effect was observed for wild-type MscL. Consistent with data shown in Fig. 4, the effects of Zn^{2+} were greater for G26H than for V23H. In addition, changes were observed at submicromolar concentrations only for G26H (Fig. 5 *B*). These data are

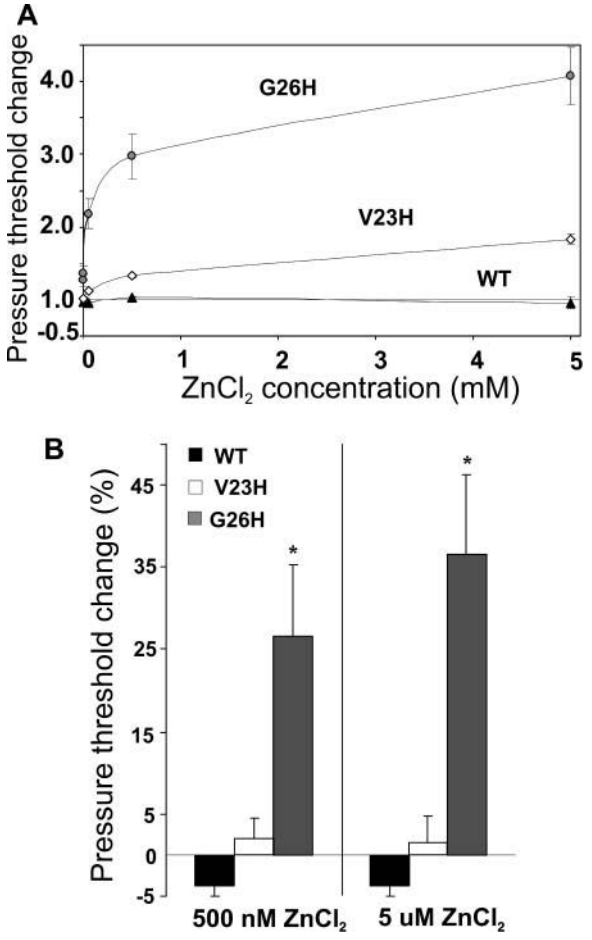

FIGURE 5 The affinity of Zn^{2+} binding to histidine mutants suggests that G26, not V23, forms the constriction point in the closed state. (*A*) The change of the pressure needed to gate WT (*solid triangles*), V23H (*open diamonds*), and G26H (*shaded circles*) MscL, as a function of metal ion concentration, is shown. The pressure thresholds were measured in patch-clamp experiments at increasing concentrations of Zn^{2+} ion applied to the bath. Error bars are the SEM of six or more independent experiments. *(B)* Percent increases in the pressure threshold of WT (*solid*), V23H (*open*), and G26H (*shaded*) MscL after applying 500 nM (*left*) or 5 μM (*right*) Zn^{2+} to the bath (pH 8.0) are shown. Error bars are the SEM of seven or more independent experiments. $*p < 0.01$ from a paired Student's *t*-test, control versus treated. A comparison of the ratios (treated/control) at both concentrations also showed a significant difference between G26H versus WT ($*p < 0.01$ from an unpaired Student's *t*-test).

consistent with G26 forming a constriction point in the closed state of the MscL channel.

Two metals having different radii exert opposite effects on L19H

Similar to all cases noted above, Cd^{2+} increased pressure threshold of the L19H mutant. In contrast, after treatment with Ni^{2+}, lower pressures were sufficient for channel gating (Fig. 6, *A* and *B*) in a dose-dependent manner (Fig. 6 *B*). Furthermore, spontaneous activity was frequently observed subsequent to the addition of Ni^{2+} (12 of 23 patches). Spontaneous activity was never observed in 89 independent L19H patches in the absence of Ni^{2+}. All of these effects were reversible and observed at pH 8.0 but not at pH 6.0 with all Ni^{2+} concentrations tested (not shown). Hence, Ni^{2+} and Cd^{2+} exert opposing effects on L19H gating.

DISCUSSION

Metal binding to endogenous and substituted cysteines and histidines has been used to elucidate the mechanisms of gating of the Shaker voltage-activated K^+, hyperpolarization-activated cation, and cyclic nucleotide-gated channels (Holmgren et al., 1998; Rothberg et al., 2002, 2003; Webster et al., 2004). Here, we have used a similar approach to determine the relative position of residues within the pore of MscL. Our data help define the residues within the channel lumen and support a model for structural transitions that occur during gating.

Previous studies using random and site-directed mutagenesis have found that mutations within TM1 of MscL alter channel properties (Blount et al., 1996a, 1997; Ou et al., 1998; Yoshimura et al., 1999; Maurer and Dougherty, 2003). One study at position G22 demonstrated that the ability to confer a GOF phenotype, a decrease in pressure threshold of the channel, and a shorter open dwell time all correlated with the hydrophilicity of the substitution at this site (Yoshimura et al., 1999). We initially selected residues for histidine substitution that have been predicted to reside within the closed or opening pore of the channel (Bartlett et al., 2004). The observation that all of these histidine mutations confer a GOF phenotype and have lower tension thresholds is consistent with this prediction. In addition, these histidine mutations also lead to channels with shorter open dwell times, consistent with the hypothesis that residues at these positions go through an aqueous environment upon gating of the channel (Blount et al., 1996b, 1997; Ou et al., 1998; Bartlett et al., 2004); thus, such mutations lead to channels that traverse transition states more easily. In contrast, the F29 mutation was not predicted to be in the opening pore by Bartlett et al. Although this mutated channel did confer a GOF phenotype in vivo, it did not show a statistically significant decrease in membrane tension threshold, nor did it have the shortened open dwell times characteristic of channels with mutations within the pore.

The R13H MscL showed the interesting property of being the only mutant that conferred a pH-dependent GOF phenotype. One interpretation is that the R13 residues within the pentamer normally approach each other during channel gating leading to an electrostatic repulsion that resists this structural change. Consistent with this interpretation, a previous study demonstrated that substitution of this residue to cysteine also results in a channel that effects a GOF phenotype (Levin and Blount, 2004) manifested as a decrease in viability when subjected to osmotic downshock; this phenotype is partially remediated by the addition of a charged

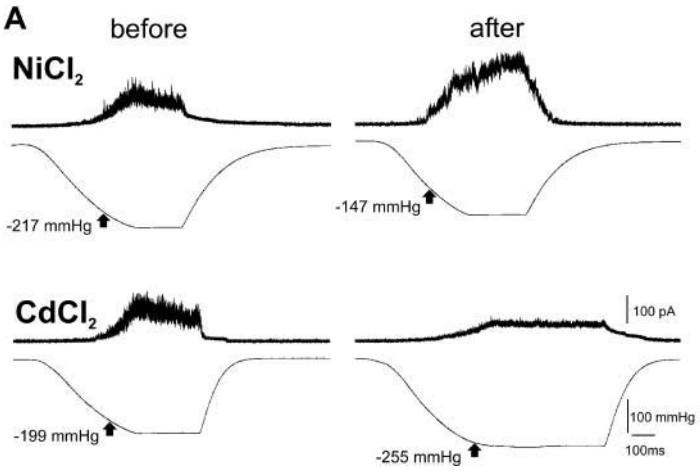

FIGURE 6 Ni^{2+} and Cd^{2+} have opposite effects on L19H gating. (*A*) Representative traces of L19H MscL activities before (*left*) and after (*right*) the addition of 5 mM Ni^{2+} or Cd^{2+} solutions to the bath (pH 8.0): the upper trace shows channel activity while the lower trace depicts the pressure applied to the patch. Arrows indicate the threshold pressure. (*B*) Changes in the pressure threshold of L19H mutant when 5 (*left*) or 50 (*right*) mM solutions of Ni^{2+} (*shaded*) and Cd^{2+} (*solid*) were added to the bath (pH 8.0). Error bars are the SEM of seven or more independent experiments. $*p < 0.01$, $**p < 0.0005$ from a paired Student's *t*-test, control versus treated.

sulfhydryl reagent (Bartlett et al., 2004). The finding presented here that the GOF phenotype is dependent upon the electrostatic state of the histidine residue further supports this hypothesis and provides a paradigm in which this mechanosensor activity can be easily ''switched'' by pH.

According to models derived from a crystallographic study, V23, or its analog in *M. tuberculosis*, V21, is predicted to form the constriction point on the periplasmic side of the channel (Chang et al., 1998; Sukharev et al., 2001b). Although the G26 residues are not predicted to face each other within the pentamer in the current models of the closed state of the channel, a cysteine substitution at this position led to a locked-closed channel that was open only after treatment with dithiothreitol; the G26C mutated channels also spontaneously formed dimers as determined by Western analysis (Levin and Blount, 2004). These findings suggested the proximity of these residues within a closed state of the channel, and that in this conformation G26, not V23, may be the constriction point. Here we find that the metal-induced inhibition of G26H gating was several-fold greater than that of V23H and was observed at much lower concentrations (effects of Zn^{2+} measured in the submicromolar range strongly suggesting metal coordination by multiple histidine residues; Fig. 5). Together, these data strongly support the hypothesis that G26, not V23, is the constriction point from the periplasmic side.

A clockwise rotation of TM1 has been previously proposed to be coupled with channel opening (Perozo et al., 2002; Bartlett et al., 2004). Here we find that metal binding to G22H, which is clockwise to G26, shows one of the largest metal-induced inhibitions, whereas V23H and I24H, which are counterclockwise, conferred less inhibition of gating (Fig. 4). Perhaps this is why metal binding inhibits gating of G22H and G26H more efficiently than V23H and I24H; the latter are counterclockwise to G26 and would only be exposed as the channel is opening and their relative distances are increasing (Fig. 7). The observation that I24H is inhibited at all by metal binding suggests that the clockwise rotation of the TM1 helix occurs early in the closed-to-open transition. An opposing model, based on molecular modeling and supported by disulfide trapping experiments, predicts a slight counterclockwise rotation of TM1 (Sukharev et al., 2001b; Betanzos et al., 2002). By this model, F29 is predicted to be within the open

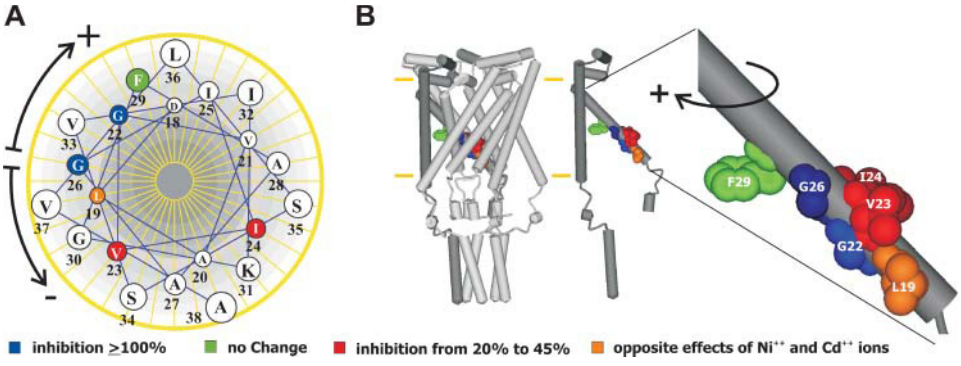

FIGURE 7 The location of the substituted residues, relative to a proposed constriction point, correlates with the degree of inhibition of channel gating by metal ions. (*A*) A model of an ideal α-helix showing residues 18–38 of TM1. Residues colored in blue, when substituted with histidine, show the greatest inhibition by metal ions. These are proposed to be the constriction point (G26) and an additional residue (G22), which is slightly clockwise to it (+ direction). A residue colored in green farther clockwise (F29) showed no change in gating properties with either of the metals. Residues colored in red (V23 and I24) show inhibition to a lesser extent. L19H, in orange, shows opposite responses to Ni^{2+} versus Cd^{2+}. (*B*) A model of the *E. coli* MscL in a closed or nearly closed structure, derived from the *M. tuberculosis* crystallographic structure, is shown (*left*). A single subunit (*middle*) and an enlargement of the relevant region of TM1 (*right*) are shown. The arrows indicate the predicted clockwise rotation of TM1 upon channel gating, opening (+), and closing (−).

pore (Sukharev et al., 2001b). Because F29 is located more toward the periplasm than the other residues tested, and within the wider region of the vestibule, the observation that metals had no effect on this mutant may be because they are not in close enough proximity, or because F29 does not lie within the pore. In either event, for this study F29 serves as an important negative control.

It is important to note that not all of the affected histidine mutants were inhibited by metal binding. The binding of Ni^{2+} to L19H lowered the threshold of this mutant, and even induced spontaneous activity in ~50% of the Ni^{2+}-treated patches. As observed with the other mutants, Cd^{2+} ions increased the pressure threshold of L19H. These opposing affects on gating observed with Ni^{2+} and Cd^{2+} ions are presumably explained by the binding to the clustered histidines in different conformations of the channel. A fundamental difference between these metals is that of ionic radius. One explanation for the observed phenomenon is that the Cd^{2+} ion binds to a conformation of the channel in which metal coordination by the histidine residues increases the energy required for gating, whereas the smaller Ni^{2+} ion interacts with the cluster by pulling it into a position that lowers the energy required for gating. Given the position of this residue (Fig. 7), this latter ''pulling'' effect could induce the tilting and/or clockwise rotation of the TM1 helices that normally heralds the gating cascade.

In conclusion, we have used the engineering of metal-binding sites to determine pore construction; an approach not previously used for MscL. Our findings have further developed a model that includes a prediction for the residues forming the constriction point of the closed channel, and those exposed early upon gating. The data support the hypothesis that G26, not V23, is the constriction point of the fully closed channel. As the authors pointed out in the original article (Chang et al., 1998), the MscL *M. tuberculosis* crystal structure, which shows V23 as the constriction point, may reflect a nearly closed, rather than a fully closed, state of the channel. Hence, the crystal structure may depict a conformation in which a slight clockwise rotation of TM1 has already occurred. In addition, the observation that residues clockwise of the constriction point are exposed, as determined by metal binding, supports a model for the clockwise rotation of TM1 early in the gating process.

The authors thank Drs. Gary Yellen and Ian Booth for helpful discussions and Jessica Bartlett and Dr. Paul Moe for critical reading of the manuscript.

This work was supported by grants GM61028 and DK60818 from the National Institutes of Health, grant I-1420 from the Welch Foundation, and grant F49620-01-1-0503 from the Air Force Office of Scientific Review.

REFERENCES

Bartlett, J. L., G. Levin, and P. Blount. 2004. An *in vivo* assay identifies changes in residue accessibility upon mechanosensitive channel gating. *Proc. Natl. Acad. Sci. USA.* 101:10161–10165.

Batiza, A. F., M. M. Kuo, K. Yoshimura, and C. Kung. 2002. Gating the bacterial mechanosensitive channel MscL *in vivo*. *Proc. Natl. Acad. Sci. USA.* 99:5643–5648.

Berrier, C., M. Besnard, B. Ajouz, A. Coulombe, and A. Ghazi. 1996. Multiple mechanosensitive ion channels from *Escherichia coli*, activated at different thresholds of applied pressure. *J. Membr. Biol.* 151:175–187.

Betanzos, M., C. S. Chiang, H. R. Guy, and S. Sukharev. 2002. A large iris-like expansion of a mechanosensitive channel protein induced by membrane tension. *Nat. Struct. Biol.* 9:704–710.

Blount, P., and P. Moe. 1999. Bacterial mechanosensitive channels: integrating physiology, structure and function. *Trends Microbiol.* 7:420–424.

Blount, P., M. J. Schroeder, and C. Kung. 1997. Mutations in a bacterial mechanosensitive channel change the cellular response to osmotic stress. *J. Biol. Chem.* 272:32150–32157.

Blount, P., S. I. Sukharev, P. C. Moe, B. Martinac, and C. Kung. 1999. Mechanosensitive channels of bacteria. *Methods Enzymol.* 294:458–482.

Blount, P., S. I. Sukharev, P. C. Moe, M. J. Schroeder, H. R. Guy, and C. Kung. 1996a. Membrane topology and multimeric structure of a mechanosensitive channel protein of *Escherichia coli*. *EMBO J.* 15:4798–4805.

Blount, P., S. I. Sukharev, M. J. Schroeder, S. K. Nagle, and C. Kung. 1996b. Single residue substitutions that change the gating properties of a mechanosensitive channel in *Escherichia coli*. *Proc. Natl. Acad. Sci. USA.* 93:11652–11657.

Chang, G., R. H. Spencer, A. T. Lee, M. T. Barclay, and D. C. Rees. 1998. Structure of the MscL homolog from *Mycobacterium tuberculosis*: A gated mechanosensitive ion channel. *Science.* 282:2220–2226.

Cherny, V. V., and T. E. DeCoursey. 1999. pH-dependent inhibition of voltage-gated H^+ currents in rat alveolar epithelial cells by Zn^{++} and other divalent cations. *J. Gen. Physiol.* 114:819–838.

Cruickshank, C. C., R. F. Minchin, A. C. Le Dain, and B. Martinac. 1997. Estimation of the pore size of the large-conductance mechanosensitive ion channel of *Escherichia coli*. *Biophys. J.* 73:1925–1931.

Epstein, W., and M. Davies. 1970. Potassium-dependent mutants of *Escherichia coli* K-12. *J. Bacteriol.* 101:836–843.

Hamill, O. P., and B. Martinac. 2001. Molecular basis of mechanotransduction in living cells. *Physiol. Rev.* 81:685–740.

Häse, C. C., A. C. Le Dain, and B. Martinac. 1995. Purification and functional reconstitution of the recombinant large mechanosensitive ion channel (MscL) of *Escherichia coli*. *J. Biol. Chem.* 270:18329–18334.

Holmgren, M., K. S. Shin, and G. Yellen. 1998. The activation gate of a voltage-gated K+ channel can be trapped in the open state by an intersubunit metal bridge. *Neuron.* 21:617–621.

Krizek, B. A., D. L. Merkle, and J. M. Berg. 1993. Ligand variation and metal-ion binding-specificity in zinc finger peptides. *Inorg. Chem.* 32: 937–940.

Levin, G., and P. Blount. 2004. Cysteine scanning of MscL transmembrane domains reveals residues critical for mechanosensitive channel gating. *Biophys. J.* 86:2862–2870.

Levina, N., S. Totemeyer, N. R. Stokes, P. Louis, M. A. Jones, and I. R. Booth. 1999. Protection of *Escherichia coli* cells against extreme turgor by activation of MscS and MscL mechanosensitive channels: identification of genes required for MscS activity. *EMBO J.* 18:1730–1737.

Li, Y., P. C. Moe, S. Chandrasekaran, I. R. Booth, and P. Blount. 2002. Ionic regulation of MscK, a mechanosensitive channel from *Escherichia coli*. *EMBO J.* 21:5323–5330.

Li, Y., R. Wray, and P. Blount. 2004. Intragenic suppression of gain-of-function mutations in the *Escherichia coli* mechanosensitive channel, MscL. *Mol. Microbiol.* 53:485–495.

Liu, Y., M. Holmgren, M. E. Jurman, and G. Yellen. 1997. Gated access to the pore of a voltage-dependent K^+ channel. *Neuron.* 19:175–184.

Maurer, J. A., and D. A. Dougherty. 2003. Generation and evaluation of a large mutational library from the *Escherichia coli* mechanosensitive channel of large conductance, MscL: implications for channel gating and evolutionary design. *J. Biol. Chem.* 278:21076–21082.

McLaggan, D., M. A. Jones, G. Gouesbet, N. Levina, S. Lindey, W. Epstein, and I. R. Booth. 2002. Analysis of the kefA2 mutation suggests that KefA is a cation-specific channel involved in osmotic adaptation in *Escherichia coli*. *Mol. Microbiol.* 43:521–536.

Moe, P. C., G. Levin, and P. Blount. 2000. Correlating a protein structure with function of a bacterial mechanosensitive channel. *J. Biol. Chem.* 275:31121–31127.

Ou, X., P. Blount, R. J. Hoffman, and C. Kung. 1998. One face of a transmembrane helix is crucial in mechanosensitive channel gating. *Proc. Natl. Acad. Sci. USA*. 95:11471–11475.

Paddock, M. L., L. Sagle, A. Tehrani, J. T. Beatty, G. Feher, and M. Y. Okamura. 2003. Mechanism of proton transfer inhibition by Cd2+ binding to bacterial reaction centers: determination of the pKA of functionally important histidine residues. *Biochemistry*. 42:9626–9632.

Perozo, E., D. M. Cortes, P. Sompornpisut, A. Kloda, and B. Martinac. 2002. Open channel structure of MscL and the gating mechanism of mechanosensitive channels. *Nature*. 418:942–948.

Rothberg, B. S., K. S. Shin, P. S. Phale, and G. Yellen. 2002. Voltage-controlled gating at the intracellular entrance to a hyperpolarization-activated cation channel. *J. Gen. Physiol*. 19:83–91.

Rothberg, B. S., K. S. Shin, and G. Yellen. 2003. Movements near the gate of a hyperpolarization-activated cation channel. *J. Gen. Physiol*. 122: 501–510.

Sukharev, S., M. Betanzos, C. Chiang, and H. Guy. 2001a. The gating mechanism of the large mechanosensitive channel MscL. *Nature*. 409: 720–724.

Sukharev, S., S. Durell, and H. Guy. 2001b. Structural models of the MscL gating mechanism. *Biophys. J*. 81:917–936.

Webster, S. M., D. del Camino, J. P. Dekker, and G. Yellen. 2004. Intracellular gate opening in Shaker K+ channels defined by high-affinity metal bridges. *Nature*. 428:864–868.

Yoshimura, K., A. Batiza, M. Schroeder, P. Blount, and C. Kung. 1999. Hydrophilicity of a single residue within MscL correlates with increased channel mechanosensitivity. *Biophys. J*. 77:1960–1972.